



Permeability of Self-Affine Fractures

V. V. MOURZENKO¹, J.-F. THOVERT¹ and P. M. ADLER²

¹LCD-PTM, SP2MI, BP 179, 86960 Futuroscope Cedex, France. e-mail: mourzenk@lcd.ensma.fr; thovert@lcd.ensma.fr

²IPGP, tour 24, 4 Place Jussieu, 75252 Paris Cedex 05, France. e-mail: adler@ipgp.jussieu.fr

(Received: 1 February 2000; in final form: 2 September 2000)

Abstract. The permeability of self-affine fractures with various roughness exponents H is investigated by direct three-dimensional numerical simulations. A scaling behavior with an exponent H is exhibited in the self-affine scale range. Permeability can be related to the fractional open area and to the percolation probability by simple models.

Key words: fracture, permeability, self-affine.

1. Introduction

The flow properties of rocks, which are very important in various problems such as nuclear waste repository or geothermal energy recovery, are greatly influenced by the presence of fractures, which act as preferential paths.

For this reason, the permeability of individual fractures has been actively studied, both experimentally and numerically. A recent review of this topic can be found in Adler and Thovert (1999). However, most of the earlier numerical investigations were based on the solution of the two-dimensional Reynolds equation (see e.g., Brown, 1989), which results from a lubrication approximation, whereas Mourzenko *et al.* (1995) showed that this model overestimates the permeability by a factor larger than 2, for realistic values of aperture and roughness, when compared to the solution of the three-dimensional Stokes equations. Volik *et al.* (1997) reached a similar conclusion for the related problem of conduction in fractures.

On the other hand, it is now well known that the surfaces of most natural fractures are self-affine over some range of length scales. Such fractures may appear macroscopically homogeneous, but scale dependence of the transport properties are expected for scales in the self-affine range. Since the Reynolds equation relies on the assumption that the fracture surfaces can be considered as locally smooth, the applicability of this model is even more questionable for self-affine than for regular fractures.

Gutfraind and Hansen (1995) used lattice gas automata to solve the local flow equations in self-affine fractures, but their investigations were restricted to two-dimensional channels, with symmetric non-contacting walls. Their observation, that permeability is governed by the height of the largest asperities regardless of

the roughness exponent, is strongly connected with their particular geometrical model. Zhang *et al.* (1996) also used lattice gas simulations to compute the flow in three-dimensional self-affine fractures, but they did not address size effects.

Finally, even though many experimental investigations are reported in the literature, they are most often difficult to analyze, since the fracture geometry is not sufficiently documented. Notable exceptions are the studies by Hakami and Barton (1990), Durham and Bonner (1994) and Plouraboué (1996). However, in all these cases, just as in the simulations of Gutfraind and Hansen (1995), contact areas were either non-existent or of negligible extent.

The present work is an extension of the previous studies of Mourzenko *et al.* (1995), who addressed mostly fractures with smooth (*i.e.*, non self-affine) surfaces, and of Mourzenko *et al.* (1999), who considered the percolation and conduction properties of self-affine fractures. This work closely follows the methodology of Mourzenko *et al.* (1999). Fractures with self-affine geometries are numerically generated, with various mean apertures, roughness amplitudes, and roughness exponents, and the Stokes equations, which rule the fluid flow at the microscale, are solved as described by Mourzenko *et al.* (1995).

Emphasis is put on fractures with moderate apertures, *i.e.*, non-vanishing fractional contact areas, which better mimic real fractures than, for instance, the first-contact assembly of rock surfaces. As shown by Mourzenko *et al.* (1999) for conductivity, peculiar properties are observed in this regime, with size scaling effects and an influence of the roughness exponent, which disappear when the aperture increases.

This problem is closely related to studies performed on the scaling properties of percolation in random surfaces with long-range correlations. Percolation properties were studied by Schmittbuhl *et al.* (1993), Sahimi and Mukhopadhyay (1996) and Marrink *et al.* (1998). In addition, the conductivity of correlated bond networks was analyzed by Sahimi and Mukhopadhyay (1996). These studies appear to be very sensitive to the definition of percolation and to the procedure which is used to analyze the results.

This paper is organized as follows. The reader will often be referred to the companion paper by Mourzenko *et al.* (1999), and many details will be skipped. Section 2 provides a general overview of the geometry of self-affine fractures and introduces a few statistical notations. Then, the flow problem is described, and the numerical procedures for the generation of the fractures, the solution of the transport problem and the statistical treatments are presented. We tried to choose the most realistic conditions and procedures, *i.e.*, the ones which would be the most easily used if a real experiment was performed. Finally, the various parameters which play a role in the problem are reviewed, together with the main expected regimes.

Section 3 summarizes the main geometrical and percolation properties of self-affine fractures, as studied by Mourzenko *et al.* (1999). The variances of the surface heights and of the fracture apertures in finite samples are quantified. Analytical

expressions are provided, which account for the influences of all the parameters, and especially for the scaling with the sample size. Several sets of statistical parameters are equivalent for describing the local geometry of a fracture. Finally, the percolation properties of self-affine fractures are recalled. The most salient feature is that the percolation probability does not depend upon the sample size. It varies smoothly from 0 to 1 as the aperture (or fractional open area) increases, and there is no percolation threshold.

The numerical results for permeability are given in Section 4. The permeability of fractures with vanishing to moderate apertures is investigated. Permeability is shown to be related by power laws to the sample size and to the fractional open area, but no critical transition is observed. The permeability can also be related to the percolation probability. These two representations are discussed in Section 5.

2. General

2.1. DESCRIPTION OF FRACTURES

The two surfaces of a fracture can be described by their heights $z = h^\pm(x, y)$ above an arbitrary reference plane $z = 0$. Usually, h^\pm are assumed to be normally distributed random variables with a variance σ_h^2 (see Mourzenko *et al.*, 1996, for details). The aperture b of the fracture is the difference $w = h^+ - h^-$ when it is nonnegative

$$b = \begin{cases} w, & w(\mathbf{r}) \geq 0, \\ 0, & w(\mathbf{r}) < 0, \end{cases} \quad (1)$$

b may be described by its mean $\langle b \rangle$ and its variance σ_b^2 , which are generally not equal to the mean separation $b_m = \langle w \rangle$ and to σ_w^2 , respectively. When w is negative, the surfaces are considered to be in contact, with $h^+ = h^-$. It is assumed here that the two surfaces are uncorrelated, which implies that $\sigma_w^2 = 2\sigma_h^2$.

The statistical properties of the fracture in the xy -plane can be characterized by the spatial covariance functions C_{h^+} and C_{h^-} of the fields h^+ and h^- . These two functions are assumed here to be identical, stationary, and isotropic. Hence, they reduce to the function $C_h(u)$ of the norm u of the lag \mathbf{u}

$$C_h(u) = \langle [h^\pm(\mathbf{r}) - \langle h^\pm \rangle][h^\pm(\mathbf{r} + \mathbf{u}) - \langle h^\pm \rangle] \rangle. \quad (2)$$

The self-affine character of many rock surfaces was demonstrated by experimental observations (see, e.g., Brown and Scholz, 1985). Their covariance C_h can be characterized by their Fourier spectrum

$$C_h(\mathbf{r}) = \int I(\mathbf{k}) e^{-2i\pi\mathbf{k}\cdot\mathbf{r}} d^2\mathbf{k}, \quad I(\mathbf{k}) \sim k^{-2H-2}, \quad 0 < H < 1. \quad (3)$$

The same three values $H = 0.25, 0.50$ and 0.87 as in Mourzenko *et al.* (1999) are considered in this paper.

2.2. NOTATIONS

In the following, we will consider subdomains Ω of a fracture F , with size λ . The spatial averages and variances over such domains are denoted by an overbar ($\bar{\cdot}$)

$$\bar{X} = \frac{1}{\Omega} \int_{\Omega} X(\mathbf{r}) d^2\mathbf{r} \quad \overline{\sigma_X^2} = \frac{1}{\Omega} \int_{\Omega} (X(\mathbf{r}) - \bar{X})^2 d^2\mathbf{r}. \quad (4)$$

For instance, the average and variance of the aperture over Ω are \bar{b} and $\overline{\sigma_b^2}$, respectively. By analogy, the hydraulic aperture of Ω will be denoted \bar{b}_h , since it is also a local average property.

Finally, conditional averages of \bar{X} over domains which share a common value y of some random variable Y are denoted $\langle \bar{X} \rangle_Y$, i.e.,

$$\langle \bar{X} \rangle_Y(y) = \frac{1}{N_y} \sum_{i=1}^{N_y} \bar{X}_i, \quad (5)$$

where N_y is the number of domains where the variable Y takes the value y . For instance, $\langle \bar{b}_h \rangle_{\bar{b}/\overline{\sigma_b}}$ is the mean hydraulic aperture of all fracture samples which have a given ratio $\bar{b}/\overline{\sigma_b}$.

2.3. FLUID FLOW MODEL

Consider a rough-walled channel with dimensions $\lambda \times \lambda$ in the x - y plane. The low Reynolds number flow of an incompressible Newtonian fluid through this channel is governed by the usual three-dimensional Stokes equations (see Mourzenko *et al.*, 1995) together with the no slip boundary condition

$$\mu \nabla^2 \mathbf{v} = \nabla p, \quad \nabla \cdot \mathbf{v} = 0, \quad \mathbf{v} = 0 \text{ on } S, \quad (6)$$

where \mathbf{v} , p , and μ are the velocity, pressure, and viscosity of the fluid, respectively, and S is the fluid–solid interface.

The permeability \bar{B}_x along the x -axis of the fracture sample is determined by solving Equation (6), when the sample is placed between upstream and downstream tanks at pressures Δp and 0, respectively, and between two impervious lateral walls. These boundary conditions are chosen since they are the ones which would be the most easily imposed in a real experiment. They correspond to the mixed boundary conditions

$$p = \Delta p \quad \text{at } x = 0 \quad (7a)$$

$$p = 0 \quad \text{at } x = \lambda \quad (7b)$$

$$\mathbf{v} = 0 \quad \text{at } y = 0 \text{ and } \lambda \quad (7c)$$

The average flow rate \bar{Q} per unit channel width may be defined as

$$\bar{Q} = \frac{1}{\lambda^2} \int_{\tau_f} \mathbf{v} d^3\mathbf{r}. \quad (8)$$

The permeability \overline{B}_x of the fracture is deduced from the x -component \overline{Q}_x of \mathbf{Q}

$$\overline{Q}_x = -\frac{\overline{B}_x}{\mu} \frac{\Delta p}{\lambda}. \quad (9)$$

Finally, the hydraulic aperture \overline{b}_h , which has the dimension of a length, is defined as

$$\overline{b}_h = (12\overline{B}_x)^{1/3}. \quad (10)$$

It may be viewed as the aperture of an equivalent plane channel, which yields the same flux \overline{Q}_x under the same conditions (7). Additional details can be found in Mourzenko *et al.* (1995).

2.4. NUMERICAL PROCEDURE

The permeability of self-affine fractures is investigated by considering finite samples cut from fractures generated with a larger size.

Square fractures of size $\mathcal{L} \times \mathcal{L}$ are reconstructed, by generating the heights h^+ and h^- at the nodes $(i\Delta x, j\Delta y)$ of a regular square grid with $\Delta x = \Delta y = a$, $\mathcal{L} = \mathcal{N}_c a$ and $i, j = 1, 2, \dots, \mathcal{N}_c$.

The random fields h^+ and h^- are generated by the standard method of Fourier transforms (see Adler, 1992, and Mourzenko *et al.*, 1996, for details), by imposing their variance σ_h^2 and the power spectrum of the covariance C_h

$$\frac{I(\mathbf{k})}{I(0)} = \begin{cases} \|\mathbf{k}\Lambda\|^{-2H-2}, & \|\mathbf{k}\Lambda\| > 1 \\ 1, & \|\mathbf{k}\Lambda\| \leq 1. \end{cases} \quad (11)$$

The normalization constant $I(0)$ is set so that the integral of the power spectrum equals the variance σ_h^2 . The length scale $\Lambda = n_\Lambda a$ is the upper cut-off for the self-affinity of the surface profiles.

Once the profiles h^+ and h^- are obtained, the fracture geometry is constructed for a given separation b_m . Then the fracture is discretized by a three-dimensional array of elementary cubes of size a , filled either with fluid or solid. The grid resolution is set to $a = \sigma_h/5$.

A square domain of size $\lambda = n_\lambda a$ is then cut from this master sample. The separation b_m is adjusted so that the fractional open area \overline{S}_0 in the subdomain is equal to some prescribed value, and its hydraulic aperture is computed by solving the problem (6–10).

Then new fractures are generated in order to build a statistical set, over which the average hydraulic aperture is evaluated. This corresponds to the statistical procedure (iii a) in the Appendix of Mourzenko *et al.* (1999). Generally, the number \mathcal{N}_r of random realizations for each case is at least 100; it was increased up to several thousands in some cases when the probability of percolation is small, so that the statistical set contains at least several tens of percolating configurations;

it was slightly decreased for the largest samples ($\mathcal{N}_r \geq 50$, for $n_\lambda \geq 128$), owing to the length of the computations.

As a general rule, $\mathcal{N}_c = 1024$ and $n_\Lambda = 512$. The large ratio $\Lambda/a = 512$ ensures that a wide range of scales λ exists, between the size a of the smallest features of the surfaces which can be represented, and the upper cut-off length Λ of the self-affinity,

$$1 \ll n_\lambda \ll n_\Lambda \quad \text{or} \quad a \ll \lambda \ll \Lambda. \quad (12)$$

The results presented in the following correspond to $32 \leq n_\lambda \leq 160$.

2.5. OVERVIEW OF THE PARAMETERS

Five dimensionless parameters may a priori play a role in the problem at hand, namely the exponent H , the ratio of the mean separation to the surface roughness b_m/σ_h , the relative size of the domains λ/Λ , the discretization parameter a/σ_h and the ratio Λ/a . Since we are interested in this paper in the hydraulic properties of finite regions of a self-affine fracture, in the self-affinity range $a \ll \lambda \ll \Lambda$, the influence of the numerical cut-off lengths a and Λ vanishes. The first two parameters are the basic geometrical characteristics of the fracture. In the self-affine range the permeability of finite samples is expected to depend on their size λ .

3. Geometrical Properties

We summarize in this Section some of the geometrical properties established by Mourzenko *et al.* (1999).

For any finite domain with size $\lambda \ll \Lambda$, cut from a larger fracture generated as described in Subsection 2.4, the mean separation \bar{w} , the mean aperture \bar{b} , the fractional open area \bar{S}_0 and the variances $\bar{\sigma}_b^2$ and $\bar{\sigma}_h^2$ of the aperture and surface elevation are defined from simple spatial statistics, denoted by the overbars.

The averages \bar{w} , \bar{b} and \bar{S}_0 do not depend on the sample size λ , and their statistical expectations are obviously equal to the overall averages

$$\langle \bar{w} \rangle = b_m, \quad \langle \bar{b} \rangle = \langle b \rangle, \quad \langle \bar{S}_0 \rangle = S_0. \quad (13)$$

However, due to the self-affine character of the fracture, the variances $\bar{\sigma}_b^2$ and $\bar{\sigma}_h^2$ are expected to increase with λ . Mourzenko *et al.* (1999) showed that their expectations Σ_b^2 and Σ_h^2 scale according to the power laws

$$\Sigma_h^2 \approx \sigma_h^2 \Theta(H) Q(H) \left(\frac{\lambda}{\Lambda} \right)^{2H_h}, \quad \left(\frac{\lambda}{\Lambda} \right)^{2-2H} \ll 1, \quad (14a)$$

$$\Sigma_b^2 \approx 2S_0 \Sigma_h^2, \quad \left(\frac{\lambda}{\Lambda} \right)^{2H} \ll 1, \quad (14b)$$

where the functions Θ and Q depend on H only. The exponent H_h is close to H , but slightly shifted towards $1/2$ ($H_h = 0.30, 0.50$ and 0.79 , for $H = 0.25, 0.50$ and 0.87 , respectively), due to the band-limited character of the spectral density function (11) (see Kant, 1996; Mourzenko *et al.*, 1999).

As a consequence of the Gaussian character of the surface heights, the statistical properties of finite pieces of fractures with a prescribed ratio of local mean separation and surface roughness $\bar{w}/\bar{\sigma}_h$ are given by

$$\langle \bar{S}_0 \rangle_{\bar{w}/\bar{\sigma}_h} = \frac{1}{2} \operatorname{erfc} \left(-\frac{\bar{w}}{2\bar{\sigma}_h} \right), \quad (15a)$$

$$\left\langle \frac{\bar{b}}{\bar{\sigma}_h} \right\rangle_{\bar{w}/\bar{\sigma}_h} = \langle \bar{S}_0 \rangle_{\bar{w}/\bar{\sigma}_h} \frac{\bar{w}}{\bar{\sigma}_h} + \frac{1}{\sqrt{\pi}} e^{-\bar{w}^2/4\bar{\sigma}_h^2}, \quad (15b)$$

$$\left\langle \frac{\bar{\sigma}_b^2}{\bar{\sigma}_h^2} \right\rangle_{\bar{w}/\bar{\sigma}_h} = \langle \bar{S}_0 \rangle_{\bar{w}/\bar{\sigma}_h} \left(2 + \frac{\bar{w}^2}{\bar{\sigma}_h^2} \right) + \frac{\bar{w}}{\sqrt{\pi}\bar{\sigma}_h} e^{-\bar{w}^2/4\bar{\sigma}_h^2} - \left\langle \frac{\bar{b}}{\bar{\sigma}_h} \right\rangle_{\bar{w}/\bar{\sigma}_h}^2. \quad (15c)$$

Furthermore, the domain size λ has absolutely no influence; whatever λ/Λ , $\langle \bar{b}/\bar{\sigma}_h \rangle_{\bar{w}/\bar{\sigma}_h}$ or $\langle \bar{\sigma}_b^2/\bar{\sigma}_h^2 \rangle_{\bar{w}/\bar{\sigma}_h}$ are identical for identical $(\bar{w}/\bar{\sigma}_h)$.

Therefore, the statistical geometry of subdomains of a fracture is fully characterized by the two parameters $\bar{\sigma}_h$ and $\bar{w}/\bar{\sigma}_h$, with all the scale effects embodied in the scaling law (14a) for $\bar{\sigma}_h$. Alternatively, $\bar{\sigma}_b$ and $\bar{b}/\bar{\sigma}_b$ or \bar{S}_0 can be used instead of $\bar{\sigma}_h$ and $\bar{w}/\bar{\sigma}_h$ to describe the geometry, since the two sets of parameters are related by (15). In the following, the fracture local permeabilities will be systematically analyzed in terms of \bar{b} , $\bar{\sigma}_b$ and \bar{S}_0 .

Finally, Mourzenko *et al.* (1999) considered the percolation probability of finite samples of self-affine fractures of size λ , according to the rule \mathcal{R}_1 as defined by Reynolds *et al.* (1980). The most striking observation was that the percolation probability $P(\bar{S}_0, \lambda)$ is actually independent of the sample size λ , provided it is in the self-affine range, $a \ll \lambda \ll \Lambda$.

4. Permeability

The permeability of self-affine fractures with $H = 0.25, 0.50$ and 0.87 and \bar{S}_0 from 0.1 to 0.8 was computed over domains of varying size λ , with $\lambda \ll \Lambda$. The discretization $a/\sigma_h = 0.2$ was used in all calculations. As it is shown by Mourzenko *et al.* (1999), such a resolution is sufficient for the problem under consideration.

In this study, the local permeabilities are analyzed in relation with the local geometrical characteristics. They were averaged over domains with identical \bar{S}_0 .

Recall the two main observations of Mourzenko *et al.* (1999) relative to the conductivity C of self-affine fractures. In the first place, they showed that the scale effects were fully accounted for by the normalization of the conductivity by the

local aperture standard deviation $\overline{\sigma}_b$. Then, two power laws were obtained, in terms of the reduced mean local aperture and of the local fractional open area

$$\langle \overline{C}/\overline{\sigma}_b \rangle_{\overline{b}/\overline{\sigma}_b} \propto (\overline{b}/\overline{\sigma}_b - b^*)^{\alpha_{C,b}}, \quad (16a)$$

$$\langle \overline{C}/\overline{\sigma}_b \rangle_{S_0} \propto \overline{S}_0^{\alpha_{C,S}}. \quad (16b)$$

The offsets b^* in (16a) were set in order to obtain the best alignment of the conductivity data for each exponent H , namely $b^* = 0.23, 0.22$ and 0.29 for $H = 0.25, 0.50$ and 0.87 , respectively. The exponent $\alpha_{C,S}$ was found very close to $5 - 3H$.

The same analysis was conducted here for permeability. However, it must be noticed that the average of the hydraulic apertures on a statistical set can differ from the hydraulic aperture deduced from the mean permeability on the same set. In particular, this difference can depend on the fraction $P(\overline{S}_0)$ of percolating samples. It is easily seen that

$$\left\langle \frac{\overline{b}_h}{\overline{\sigma}_b} \right\rangle = P(\overline{S}_0) \left\langle \frac{\overline{b}_h}{\overline{\sigma}_b} \right\rangle_c, \quad (17a)$$

$$\left\langle \frac{\overline{b}_h^3}{\overline{\sigma}_b^3} \right\rangle = P(\overline{S}_0) \left\langle \frac{\overline{b}_h^3}{\overline{\sigma}_b^3} \right\rangle_c, \quad (17b)$$

where $\langle \cdot \rangle_c$ refers to an average over the percolating realizations only. Consequently,

$$\frac{\langle (\overline{b}_h/\overline{\sigma}_b)^3 \rangle}{\langle \overline{b}_h/\overline{\sigma}_b \rangle^3} = \frac{1}{P^2(\overline{S}_0)} \frac{\langle (\overline{b}_h/\overline{\sigma}_b)^3 \rangle_c}{\langle \overline{b}_h/\overline{\sigma}_b \rangle_c^3}. \quad (18)$$

For all the cases considered in these calculations, the ratio in the right-hand side of (18) was found to vary in a narrow range

$$1.0 \leq \frac{\langle (\overline{b}_h/\overline{\sigma}_b)^3 \rangle_c^{1/3}}{\langle \overline{b}_h/\overline{\sigma}_b \rangle_c} \leq 1.2. \quad (19)$$

Hence, the hydraulic aperture deduced from the mean permeability is related to the mean of the hydraulic apertures by

$$\langle (\overline{b}_h/\overline{\sigma}_b)^3 \rangle^{1/3} \approx 1.1 P(\overline{S}_0)^{-2/3} \langle \overline{b}_h/\overline{\sigma}_b \rangle \pm 10\%. \quad (20)$$

Examples of distributions of $\overline{b}_h/\overline{\sigma}_b$ for the percolating fractures for various values of H , N_c and S_0 , are shown in Figure 1, with a comparison of $\langle \overline{b}_h/\overline{\sigma}_b \rangle_c$ and $1/1.1 \langle (\overline{b}_h/\overline{\sigma}_b)^3 \rangle_c^{1/3}$.

Data for $\langle \overline{b}_h/\overline{\sigma}_b \rangle$ are plotted against the fractional open area S_0 in Figure 2. For clarity, the data for $H = 0.5$ and 0.87 were shifted by one and two decades vertically, respectively. It appears again that the data for various domain sizes are well gathered by this representation, which means that the scale effects on permeability are fully accounted for by the normalization of the hydraulic aperture by the local

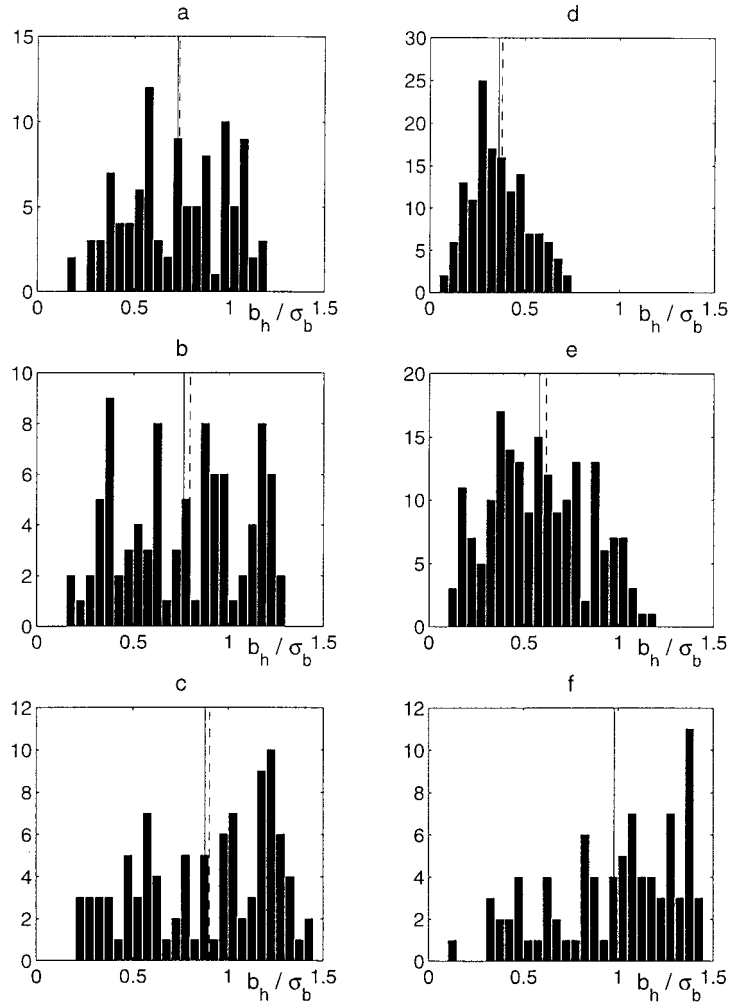


Figure 1. Histograms of the reduced hydraulic apertures $\overline{b_h / \sigma_b}$ in the percolating fractures for $H = 0.87$, $N_c = 96$ and $S_0 = 0.3, 0.5$ and 0.7 (a, b, c), and for $N_c = 64$, $S_0 = 0.7$ and $H = 0.25, 0.50$ and 0.87 (d, e, f). The vertical lines are the averages $\langle \overline{b_h / \sigma_b} \rangle_c$ (—) and $1/1.1 \langle (\overline{b_h / \sigma_b})^3 \rangle_c^{1/3}$ (---).

aperture standard deviation $\overline{\sigma_b}$. The data for different n_λ gather fairly well around straight lines without any adjustable parameter. Least square fits of the data for $N_c = 96$ yield

$$\langle \overline{b_h / \sigma_b} \rangle = 1.80 \overline{S_0}^{4.34} \quad H = 0.25, \quad (21a)$$

$$\langle \overline{b_h / \sigma_b} \rangle = 1.96 \overline{S_0}^{3.52} \quad H = 0.50, \quad (21b)$$

$$\langle \overline{b_h / \sigma_b} \rangle = 1.77 \overline{S_0}^{2.58} \quad H = 0.87. \quad (21c)$$

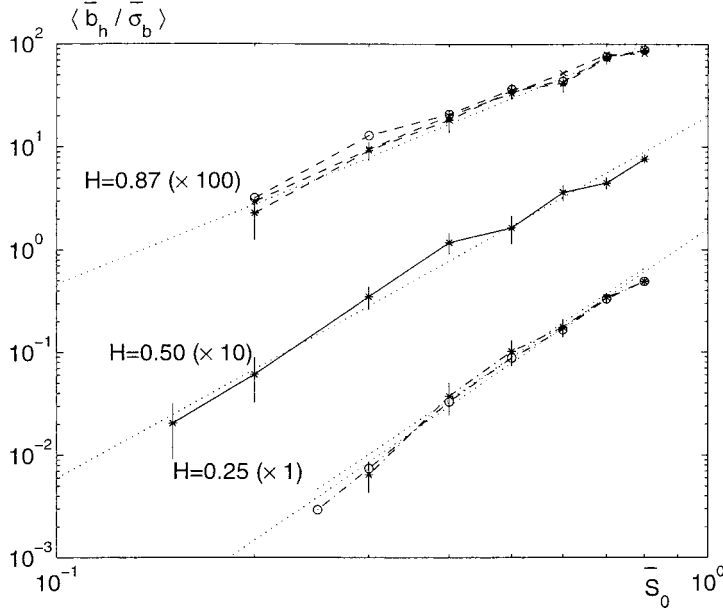


Figure 2. Loglog plot of the reduced hydraulic aperture $\langle \bar{b}_h / \bar{\sigma}_b \rangle_{\bar{S}_0}$ for self-affine fractures with $H = 0.87$ (---), 0.50 (—) and 0.25 (- · - · -), and $n_\lambda = 32$ (o), 64 (×) or 96 (*), versus \bar{S}_0 . For clarity, the data for $H = 0.5$ and 0.87 were shifted by one and two decades vertically, respectively. The dotted lines correspond to the power law fits Equation (21). Vertical lines are 95% confidence intervals.

The exponents in Equation (21) are very close to $5 - 3H$, as was $\alpha_{C,S}$ in Equation (16b). Note that a fit of the same data in the form of Equation (16a) and with the same values of b^* is also possible.

On the other hand, the average hydraulic apertures $\langle \bar{b}_h / \bar{\sigma}_b \rangle_c$ and $\langle (\bar{b}_h / \bar{\sigma}_b)^3 \rangle_c^{1/3}$ for the percolating realizations are plotted as functions of \bar{S}_0 in Figure 3. The variations of these quantities are remarkably small, compared to the variations of $\langle \bar{b}_h / \bar{\sigma}_b \rangle$ by about two orders of magnitude in Figure 2, over the range of fractional open area $S_0 = 0.2 \sim 0.7$, which corresponds to a range of relative apertures $\bar{b} / \bar{\sigma}_b = 0.4 \sim 1.04$ and to percolation probabilities from less than 0.01 to more than 0.8, when $N_c = 96$ (see Mourzenko *et al.*, 1999). Furthermore, the two types of averages yield almost identical results. It is tempting to identify the typical values of the mean hydraulic apertures with the corresponding exponent H_h (see Equation 14a), to obtain the very simple approximate model

$$\langle \bar{b}_h / \bar{\sigma}_b \rangle_c \approx H_h, \quad \langle \bar{b}_h / \bar{\sigma}_b \rangle \approx H_h P(\bar{S}_0), \quad (\pm 25\%, \quad 0.2 \leq S_0 \leq 0.7). \quad (22)$$

It was checked that the mean geometrical characteristics of the percolating realizations do not differ significantly from the overall averages, even for small values of \bar{S}_0 . For instance, with $N_c = 96$, the mean reduced apertures $\langle \bar{b} / \bar{\sigma}_b \rangle$ and $\langle \bar{b} / \bar{\sigma}_b \rangle_c$

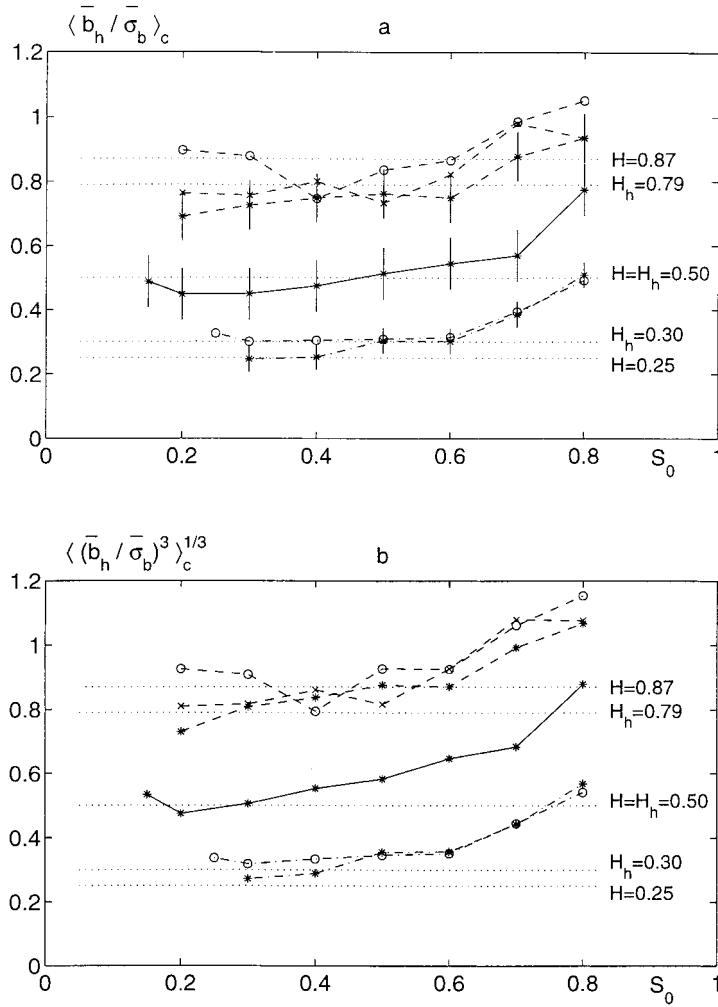


Figure 3. Average hydraulic apertures $\langle \bar{b}_h / \bar{\sigma}_b \rangle_c$ (a) and $\langle (\bar{b}_h / \bar{\sigma}_b)^3 \rangle_c^{1/3}$ (b) for the percolating realizations as functions of the fractional open area S_0 , for self-affine fractures with $H=0.87$ (---), 0.50 (—) and 0.25 (- · - · -), and $n_\lambda=32$ (o), 64 (x) or 96 (★). The horizontal dotted lines correspond to the exponents H and H_h (see Equation 14a). Vertical lines in (a) are 95% confidence intervals.

are found identical, within the statistical uncertainties, and the ratio $\langle \bar{b} \rangle_c / \langle \bar{b} \rangle$ never exceeds 1.2, for $\bar{S}_0 \geq 0.2$.

5. Discussion

Hence, two models with different functional forms have been shown to successfully describe the permeability of fractures in the self-affine regime, namely Equations (21) and (22), which relate permeability to the fractional open area and

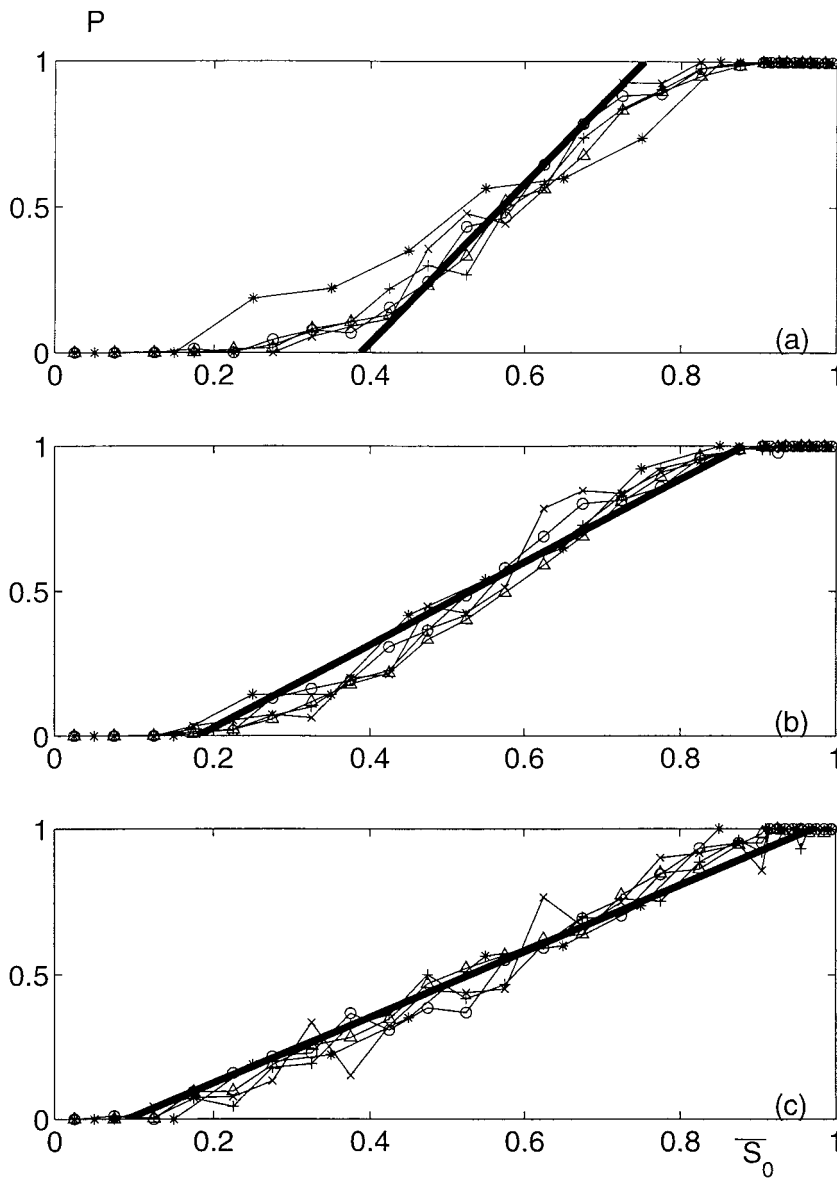
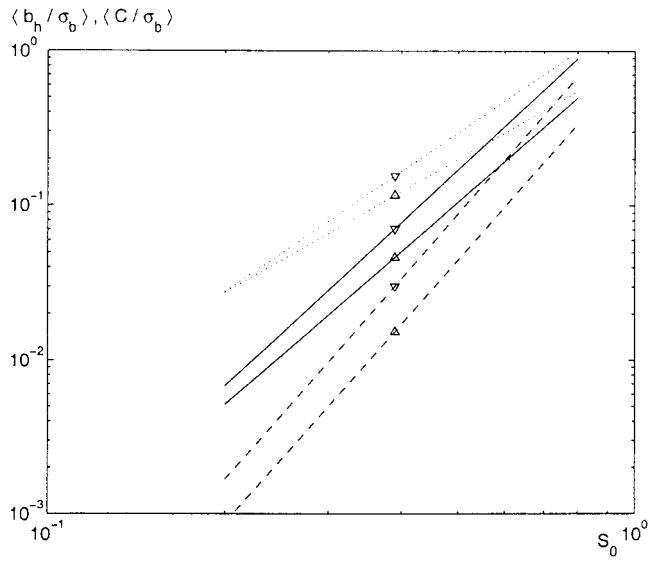


Figure 4. Percolation probability $P(\overline{S}_0, \lambda)$ as a function of the fractional open area \overline{S}_0 for $H=0.25$ (a), 0.50 (b) and 0.87 (c). Data are for $n_\lambda = 8$ (Δ), 16 ($+$), 32 (\circ), 64 (\times) and 128 (\star). The heavy lines are Equation (24).

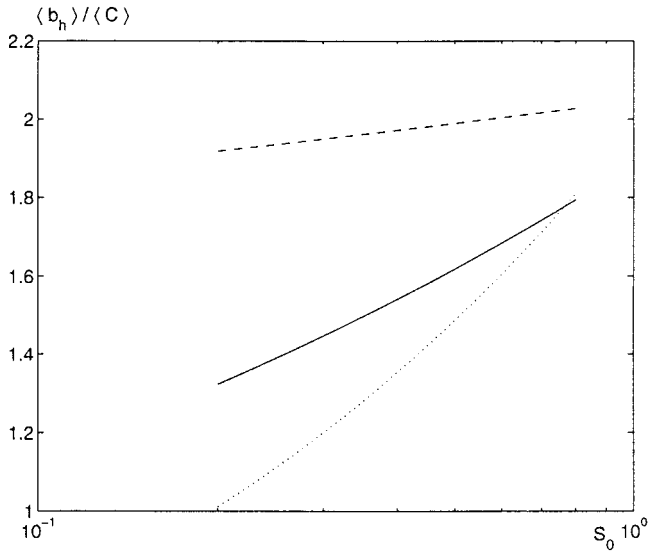
percolation probability, respectively. In both cases, the influence of the sample size is embedded in the scaling of $\overline{\sigma}_b$ with λ , given by Equation (14).

The comparison of (21) and (22) implies the surprising result

$$P(\overline{S}_0) \propto \frac{1}{H_h} \overline{S}_0^{5-3H}. \quad (23)$$



a



b

Figure 5. Hydraulic aperture $\langle \bar{b}_h / \bar{\sigma}_b \rangle$ (Δ) and electrical aperture $\langle \bar{b}_e / \bar{\sigma}_b \rangle = \langle \bar{C} / \bar{\sigma}_b \rangle$ (∇), as given by Equations (21, 16b), as functions of the fractional open area \bar{S}_0 (a). Ratio $\langle \bar{b}_h \rangle / \langle \bar{C} \rangle$ (b). Data are for self-affine fractures with $H=0.25$ (---), 0.50 (—) and 0.87 (····).

Of course, such a relationship cannot be valid over the whole range of fractional open area. It turns out, however, that a linearization of (23) around the transition fractional area $S_{0,av}$, where $P(S_{0,av}) = 1/2$, is a fair approximation of $P(\bar{S}_0)$ in the

middle range of $\overline{S_0}$.

$$P(\overline{S_0}) \approx \frac{1}{2} + \frac{5 - 3H}{H} S_{0,av}^{4-3H} (\overline{S_0} - S_{0,av}). \quad (24)$$

This result, with the values of $S_{0,av}$ given by Mourzenko *et al.* (1999), is compared in Figure 4 to the numerical data for $P(\overline{S_0})$.

As mentioned in the Introduction, there are no data in the literature which can be directly compared to the present results. The dependence of permeability on the sample size was never directly addressed, unlike, for instance, the size scaling of the mechanical properties (see, e.g., Barton and Choubey, 1977). In addition, most investigations were conducted with little control of the fracture geometry, or for vanishing fractional contact areas, where the cubic law applies with small correction factors, proportional to the surface roughness. The measurements of Durham and Bonner (1994) cover the whole range of S_0 , and show that this law breaks down when the contact area exceeds a few percents.

An interesting comparison can be made with the data of Stesky (1986), who simultaneously measured the conductivity and permeability of various artificial rock fractures. The aperture was varied by varying the normal load. The precise apertures and surface characteristics are not known, but the contact area never exceeded 0.05. From his permeability and conductivity data, the ratio $\overline{b_h}/\overline{b_e}$ of the hydraulic aperture to the electrical aperture (i.e., \overline{C}) can be evaluated, and it is always found slightly smaller than unity (0.96 ± 0.01).

In contrast, the same ratio in the present self-affine fractures is always found larger than 1. Unfortunately, the numerical computations of Mourzenko *et al.* (1999) and the present ones were not conducted with the same samples, and a direct comparison is not possible. However, the power law fits (16b) and (21) can be compared. They are both plotted as functions of $\overline{S_0}$ in Figure 5(a), and their ratio is shown in Figure 5(b). It appears that $\overline{b_h}/\overline{C}$ increases significantly, up to about 2, when H decreases, i.e., when the surfaces become more irregular.

Acknowledgements

Most computations were performed at CINES (Montpellier), subsidized by the MENESR, whose support is gratefully acknowledged.

References

- Adler, P. M.: 1992, *Porous Media: Geometry and Transports*, Butterworth/Heinemann, Stoneham, MA.
- Adler, P. M. and Thovert, J.-F.: 1999, *Fractures and Fracture Networks*, Kluwer, Dordrecht, The Netherlands.
- Barton, N. and Choubey, V.: 1977, The shear strength of rock joints in theory and practice, *Rock Mech.* **10**, 1–54.

- Brown, S. R. and Scholz, C. H.: 1985, Broad bandwidth study of the topography of natural rock surfaces, *J. Geophys. Res.* **90**, 12575–12582.
- Brown, S. R.: 1989, Transport of fluid and electric current through a single fracture, *J. Geophys. Res.* **94**, 9429–9438.
- Durham, W. B. and Bonner, B.P.: 1994, Self-propping and fluid flow in slightly offset joints at high effective pressures, *J. Geophys. Res.* **99**, 9391–9399.
- Gutfraind, R. and Hansen, A.: 1995, Study of fracture permeability using lattice gas automata, *Transport in Porous Media* **18**, 131–149.
- Hakami, E. and Barton, N.: 1990, Aperture measurements and flow experiments using transparent replicas of rock joints, in: Barton and Stephansson (Eds), *Rock Joints*, Balkema, Rotterdam, pp. 383–390.
- Kant, R.: 1996, Statistics of approximately self-affine fractals: random corrugated surface and time series, *Phys. Rev.* **B 53**, 5749–5763.
- Marrink, S. J., Paterson, L. and Knackstedt, M. A.: 2000, Definition of percolation thresholds on self-affine surface, *Physica A* **280**, 207–214.
- Mourzenko, V. V., Thovert, J.-F. and Adler, P. M.: 1995, Permeability of a single fracture; Validity of the Reynolds equation, *J. Phys. II* **5**, 465–482.
- Mourzenko, V. V., Thovert, J.-F. and Adler, P. M.: 1996, Geometry of simulated fractures, *Phys. Rev. E* **53**, 5606–5626.
- Mourzenko, V. V., Thovert, J.-F. and Adler, P. M.: 1999, Percolation and conductivity of self-affine fractures, *Phys. Rev. E* **59**, 1–20.
- Plouraboué, F.: 1996, *Propriétés géométriques et propriétés de transport des fractures à parois rugueuses*, Ph.D. Thesis, Université Paris VII, France.
- Reynolds, P. J., Stanley, H. E. and Klein, W.: 1980, *Phys. Rev. B* **21**, 1223–1245.
- Sahimi, M. and Mukhopadhyay, S.: 1996, Scaling properties of a percolation model with long-range correlations, *Phys. Rev. E.*, **54**, 3870–3880.
- Schmittbuhl, J., Sornette, J.-P. and Roux, S.: 1993, Percolation through self-affine surfaces, *J. Phys. A* **26**, 6115–6133.
- Stesky, R. M.: 1986, Electrical conductivity of brine saturated rock, *Geophysics* **51**, 1585–1593.
- Volik, S., Mourzenko, V. V., Thovert, J.-F. and Adler, P. M.: 1997, Thermal conductivity of a single fracture, *Transport in Porous Media* **27**, 305–325.
- Zhang, X., Knackstedt, M. A. and Sahimi, M.: 1996, Fluid flow across mass fractals and self-affine surfaces, *Physica A* **233**, 835–847.